

Analysis of the Mechanical Properties of Anodized Al-Si Alloys

Natal Nerímio Regone^{a*} , Célia Marina Alvarenga Freire^b, Margarita Ballester^b,

Neide Aparecida Mariano^c , Eduardo Norberto Codaro^d , Heloisa Andréa Acciari^d 

^aUniversidade Estadual Paulista, São João da Boa Vista, SP, Brasil.

^bUniversidade Estadual de Campinas, Faculdade de Engenharia Mecânica, Campinas, SP, Brasil.

^cUniversidade Federal de Alfenas, Poços de Caldas, MG, Brasil.

^dUniversidade Estadual Paulista, Escola de Engenharia, Departamento de Química e Energia, Guaratinguetá, SP, Brasil.

Received: January 28, 2022; Revised: April 11, 2022; Accepted: June 21, 2022

Aluminum alloys have been widely used in multiple applications, such as in civil construction and engine pistons. They are subjected to loads that may impair their mechanical properties. Thereby, this research aims to study the influence of anodization on the mechanical properties of alloy samples and evaluate the behavior of oxide films when subjected to tensile testing. The mechanical properties of specimens have been evaluated based on tensile and Knoop hardness tests, and strain, tensile strength, and modulus of elasticity of specimens have been determined based on the stress-strain curve. The morphology of oxide films was analyzed by scanning electron microscopy (SEM) and optical microscopy (OM). Results of anodized Al-Si alloys in both modes, i.e. pulsed and direct currents, were compared, and it was found that pulsed current was more efficient than direct current with respect to uniformity of the formed film, and that the anodization process can affect a few mechanical properties of samples. The tension testing results also revealed that the oxide film has been fractured perpendicularly towards traction. However, the oxide film hardness was not affected by the anodization mode (pulsed or direct currents). In addition, a heat treatment was efficient at improving the uniformity of anodic films.

Keywords: *Anodization, Al-Si alloys, mechanical properties, hardness.*

1. Introduction

Anodized aluminum has been successfully applied by aeronautical industries due to its high resistance to corrosion¹⁻³ and wear, and also on account of the excellent adhesion of anodic films to metallic substrates, which acts as an intermediate layer for a posterior use in painting⁴. Anodic films usually consist of two layers: a porous layer and a barrier layer which is grown during the initial process of oxide growth, while a porous layer is generated through a dissolution process of oxide films⁵. Hard anodization⁶ is employed as surface treatment for aluminum alloys at high current density and low temperatures⁷.

Pulsed current anodization offers some advantages if compared to direct current, such as shorter anodization time⁸ and better coloring of anodized aluminum⁹. The pulsed current is based on duty cycle (DC), time on (ton), time off (toff), frequency (f), average current (ia), and maximum current (im) in the period. Duty cycle is calculated from $DC = \frac{ton}{ton+toff}$, $f = \frac{1}{ton+toff} = 1/T$, $ia = im * DC$ ^{10,11}. The standard deviation of the thickness of films formed at constant voltage is smaller than that obtained by pulsed current. However, the thickness of coating growth by pulsed current was approximately twice as much as the one formed at constant voltage¹². Greater hardness of an anodic layer can be achieved by reducing temperature and using pulsed

current¹³. A duty cycle of 50% allows forming a very uniform anodic film. Anodization in both direct and pulsed current can generate a flawless oxide film layer between the Al matrix and oxides, whose hardness is greater than 349 HV¹⁴. Pulsed current is able to generate an oxide film that reduces flaws in intermetallic areas. High voltage applied at the end of a pulsed current process produces flaws by the electric field. A flawless oxide film can be formed by 50 and 75% duty cycles within 2 to 2.5 hours of processing¹⁵.

An anodic layer produced by both direct and pulsed current anodization is highly resistant to corrosion as regards the Al 2024 alloy. In addition, microhardness and nanohardness values vary according to applied potential, thus better results have been obtained from studies carried out by other authors, in which voltage ranged from 21 to 19 V¹⁶. Regarding the impact of the amount of alumina in an anodized composite, it was found that the more alumina is added to the electrolyte, the greater the oxide film hardness will be, and that it also affects tensile strength which had greater value for the film with a higher amount of alumina. However, alumina concentration was not significant after stretching¹⁷.

Tension testing requires the use of a standard sample, which is loaded up to fracture. It is generally used to obtain the mechanical properties of metals and other materials¹⁸. When a sample is loaded, it produces a stress-strain graph,

*e-mail: natal.regone@unesp.br

which can be used to calculate strain, modulus of elasticity, tensile strength, and yield strength. With respect to Al-Si and Al-Mn alloys, optimal ultimate tensile strength results were achieved by the Al-Mn alloy with 2 wt% of Mn. The resulting thickness of the anodized Al-Mn alloy demonstrated better aspect if compared to the Al-Si alloy¹⁹.

In the anodized AlCuMg alloy, there was a slight reduction in ultimate tensile and yield strength values²⁰. Mechanical tests were carried out on Al/plastic carbon fiber samples treated by tartaric sulfuric anodization (TSA), γ -glycidoxypropyltrimethoxysilane silanization (γ -GPS), and chromic acid anodization (CAA) in order to assess adhesion and corrosion resistance. It was found that Al processed by TSA, γ -GPS and CAA presented satisfactory adhesion values, although, it was observed a decrease in tensile strength after corrosion measurements of anodized samples by TSA and γ -GPS²¹. Yoganandan conducted research about the use of Mn and V in sealing through tartaric sulfuric anodization (TSA) which was compared to chromic acid anodization (CAA). Its results showed that the mechanical properties of TSA and CAA samples were similar²².

Several researchers reported the presence of large amounts of Si particles in non-uniform layers of oxide films grown on Al-Si-Cu alloys⁷. In view of such a wide range of Al-Si alloy applications in aerospace, marine, mechanical and automotive industries, the process of plasma electrolytic oxidation has been often employed to evaluate oxide film growth on it. However, it was found that it causes oxidation of silicon particles which obstructs the passage of silicon through the layer²³. The ASM Committee described a heat treatment of an Al-Si alloy at 538 °C during 12 hours, followed by immersion in boiling water²⁴.

Anodization of Al-Si alloys (heat treated) diminishes the coefficient of friction and enhances wear resistance²⁵. Processes of heating, quenching and ageing an Al alloy (A357) have revealed regular coating and a thicker oxide layer and more silicon particles within the oxide film²⁶. Silicon particles were then merged with the anodic coating after the anodization process²⁷.

Thereby, this work aims to anodize an Al-Si alloy by both direct and pulsed current in a solution containing sulfuric and oxalic acid which was used as electrolyte. Then Al-Si alloy was sealed in water boiling. The Al-Si alloy was subjected to a heat treatment so as to dissolve the alloy elements in order to improve oxide film formation. After the treatment, aluminum specimens were anodized and were submitted to tension testing so as to calculate mechanical properties and evaluate their behavior under tension. The oxide film thickness was determined through optical microscopy and the anodic film hardness was found by Knoop indentation.

2. Material and Methods

2.1. Alloy

Al-Si alloy was used in this research work. The alloy was melted into cylindrical billets and analyzed by X-ray fluorescence in order to determine the mass percentage of its constituting elements. Table 1 describes the alloy chemical composition.

The initial anodization of Al-Si samples revealed that the oxide film has been irregular. In order to improve the morphology of films, a heat treatment was performed so as to disperse silicon particles²⁴. Then, Al-Si alloy specimens were heated in a furnace at 540 °C for 12 hours and then immersed in boiling water. It produced an oxide layer on its surface, which has been removed using a 1200 grit emery paper.

2.2. Anodization process

Al-Si alloy samples were sectioned into test specimens in accordance with ASTM E 8M-97²⁸, as showed in Figure 1.

These specimens were etched with a 1.25 mol/L NaOH solution at room temperature during 180 seconds, rinsed in distilled water and subsequently immersed in a 0.18 mol/L H₂SO₄ solution for 30 seconds, followed by immersion in the anodization solution and subsequent sealing for 1 hour in distilled boiling water.

The anodization solution composition was as follows: 1.47 mol/L of H₂SO₄ and 0.40 mol/L of C₂H₂O₄·2H₂O at 20°C. Table 2 shows anodization conditions of samples produced by direct and pulsed current.

The anodic oxidation of Al-Si samples was performed in a 5000 mL PVC vessel. The solution temperature was maintained constant through a thermostatic bath. Two sheets of lead foil with 99% purity and 25 cm² area each were utilized as counter electrodes. Its power source was a rectifier from Termocontroles Ltda for voltage modulation. It was applied duty cycle (80%) and frequency (200 Hz) through pulsed current.

2.3. Tensile testing

Al-Si samples have been prepared, shaped and tested in accordance with ASTM E 8M – 97²⁸. The tensile test was performed in an MTS 810 Test Star II servo-hydraulic testing system operating at a speed of 0.01 mm/s.

A total of ten Al-Si alloy test specimens have been used in this research: four of them underwent the tension testing

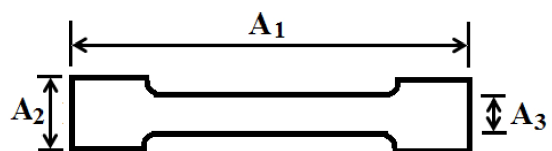


Figure 1. Shape of specimens ($A_1=120\text{mm}$, $A_2=10\text{mm}$, $A_3=6\text{mm}$).

Table 1. Al-Si alloy chemical composition determined by X-ray fluorescence (in wt%).

Al	Si	Fe	Mg	Ti	Cu	Mn	Ni
92.97	6.75	0.16	0.05	0.04	0.01	0.01	0.01

Table 2. Anodization conditions of test specimens subjected to pulsed (PC) and direct current (DC).

	Sample	Frequency (Hz)	Voltage (V)	Duty cycle (%)	Anodization time (min)	Time on (min)	Time off (min)
1	AlSiPC1	200	21	80	38	30.4	7.6
2	AlSiPC2	200	21	80	38	30.4	7.6
3	AlSiPC3	200	22	80	30	24	6
4	AlSiDC1	-	21	100	30	30	-
5	AlSiDC2	-	21	100	30	30	-
6	AlSiDC3	-	22	100	30	30	-
7	AlSiDC4 without treatment	-	18	100	30	30	-
8	AlSiDC5	-	18	100	30	30	-

(samples number 1 and 4, according to Table 2, and more two others, which were referred as AlSi WT and AlSi HT, where WT = AlSi without treatment, and HT= AlSi with heat treatment), two samples for hardness measurement (samples number 3 and 6, from Table 2), two samples for optical analysis (samples number 7 and 8 from Table 2), in addition to those used for thickness measurement (samples number 1, 2, 3, 4, 5, and 6 in Table 2). The mechanical properties of test specimens were found after examining the behavior of films.

2.4. Oxide film thickness and crack size measurements

Films have been analyzed microscopically by optical imaging using a ZEISS Neophot 32 microscope. Prior to determining film thickness, samples were embedded in resin, sandpapered with 180, 220, 320, 400, 600, 800, 1200 grit silicon carbide sandpaper and polished with 6 μm and with 1 μm diamond paste. After fracture testing, test specimens were sectioned from samples and analyzed by SEM (JEOL JXA 840A scanning electron microscope). Prior to this analysis, samples were gold-coated and micro-photographed by SEM. The size of cracks in the oxide film was calculated by a micrograph analysis of images.

2.5. Hardness measurements

Cross sections of the anodic film and heat-treated Al-Si were measured by Knoop hardness test. It involved making five indentations on each sample by applying a load of 25 g on the oxide film and of 20 g on the Al-Si matrix.

3. Results

Figures 2 and 3 show the cross section of samples, both without and with heat treatment, respectively, in order to verify the anodic film uniformity on the Al-Si substrate. Figure 2 depicts areas of silicon clusters, which can influence anodic film growth in the vicinity of these regions. Si clusters can result in flaws and decrease the oxide film thickness.

Figure 3 presents a micrograph of the AlSiDC5 sample with a uniform oxide film. Optical microscopy shows that the Al-Si matrix structure has been modified and a more uniform film was generated.

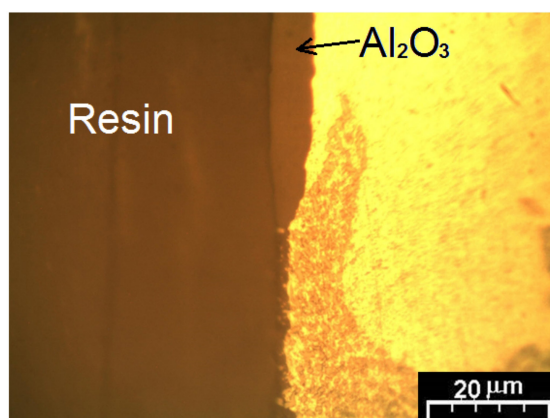


Figure 2. Optical micrograph of a cross section of the Al-Si alloy (without heat treatment) anodized by direct current (sample AlSiDC4).

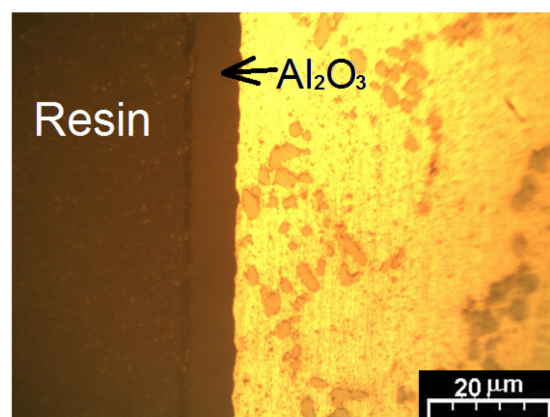


Figure 3. Optical micrograph of a cross section of the Al-Si alloy (with heat treatment) anodized by direct current (sample AlSiDC5).

Table 3 lists the thicknesses of oxide films produced by both direct and pulsed current, and their mean growth rate during current application.

The growth rate of the films was calculated when the time was on. The mean growth rate of the sample anodized by direct current varied over 30 min. In contrast, the sample produced by pulsed current showed a slightly higher growth

rate during the anodization process. Pulsed process has a constant growth rate of around $1 \mu\text{m}/\text{min}$, but the direct current process showed a growth rate ranging from 0.79 to $0.95 \mu\text{m}/\text{min}$. The anodic film thickness is related to growth rate, since the pulsed current process has a constant growth rate than the direct current process. The thickness of samples (AlSiPC1 and AlSiPC2) anodized by pulsed current are thicker than AlSiPC3, probably due to the longer anodizing time. The time on occurs when the current has achieved the maximum value, and the time off occurs when the current has achieved the minimum value. Analyzing the value around 30 min from time on, it can be noted that samples of pulsed current present thicker layers. The thickness of samples anodized by direct current (AlSiDC1 and AlSiDC2) and time on of 30 min show a difference around $4 \mu\text{m}$. This difference can be attributed to the process of direct current, because these samples have the same size. In the pulsed process performed in a shorter time on (24min-sample AlSiPC3) it was expected that there would have lower thickness. Table 4 shows the results of film thickness and tension testing of anodized and non-anodized tension specimens.

A heat treatment of the Al-Si alloy has increased strain and tensile strength and reduced yield strength to 0.1% and 0.2%, as well as the modulus of elasticity. Mg_2Si particles were factored in the hardening of heat-treated Al-Si alloys (356)²⁹. Tensile strength and yield strength values were increased by around 52% and 82%, which is associated with the heat treatment, cold work and aging and possibly enhanced precipitates (Al_3Li)³⁰. As for the Al-Li alloy, the multistep heat treatment at high temperatures and long periods boosted its strength³¹. Regarding the heat-treated alloy (Al-5Si-1Cu-Mg), it was observed a considerable ductility enhancement owing to globularization of silicon particles, the distance among them and the appearance of two phases (β'' and C) in the aging process, which resulted in exceptional mechanical properties³². The Al-12.6%Si alloy was processed by a thermomechanical treatment so as to increase its ductility. The tensile testing results showed increased elongation, i.e. close to 24%³³. There was no strain alteration in the anodized Al-Si. The anodization

process increased yield strength by 0.1% and 0.2%, as well as tensile strength.

The thicknesses of oxide layers produced by both direct and pulsed current were in the same order of magnitude. No significant differences were observed in values of tensile strength and yield strength by comparing direct current to pulsed current. However, the sample anodized by direct current showed a higher modulus of elasticity which quantifies metal hardness (stiffness). When a metal is under stress, e.g. when the modulus of elasticity is higher, elastic strain becomes insignificant¹⁸. This fact implies that anodization conducted by direct current results in lower elastic strain.

Figure 4 shows stress-strain curves of Al-Si samples. It can be observed that the area under the curve of anodized samples is larger, which indicates that anodized Al-Si is tougher, i.e. anodized Al-Si has more ability to absorb energy if compared to non-anodized Al-Si samples.

A more detailed examination in higher magnification of the partial section of samples shows that the thickness of films is represented by irregular layers, probably due to its brittleness. Figures 5 and 6 show the film images with

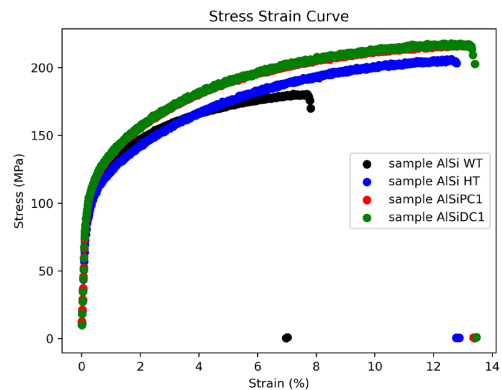


Figure 4. Stress-strain curves (Al-Si alloy with and without an anodic film) to elongation at break.

Table 3. Thickness and growth rate of films on anodized samples.

Sample	Duty cycle (%)	Anodization time (min)	Thickness (μm)	Mean Growth Rate ($\mu\text{m}/\text{min}$)	Time on (min)	Time off (min)
AlSiPC1	80	38	29.12 ± 3.48	0.96	30.4	7.6
AlSiPC2	80	38	31.94 ± 1.56	1.05	30.4	7.6
AlSiPC3	80	30	24.80 ± 2.34	1.03	24	6
AlSiDC1	100	30	28.56 ± 3.48	0.95	30	-
AlSiDC2	100	30	24.39 ± 2.65	0.81	30	-
AlSiDC3	100	30	23.81 ± 2.15	0.79	30	-

Table 4. Thickness and mechanical properties of Al-Si alloy tension specimens.

Sample	Strain (%)	Tensile strength (MPa)	Modulus of elasticity (GPa)	Yield strength at 0.1% (MPa)	Yield strength at 0.2% (MPa)	Thickness (μm)
AlSi WT	8	181	67	99	107	-
AlSi HT	13	206	62	89	102	-
AlSiPC1	13	217	63	98	113	29.12 ± 3.48
AlSiDC1	13	218	70	99	113	28.56 ± 3.48

fractures, which are perpendicular to the tension displacement, which is found by the tensile testing and indicated by arrows. The fractured bands are not uniform but occur randomly throughout the Al-Si substrate.

The fractured bands of the anodic film are separated due to the tensile process. Since the oxide film cracks, it remains adhered to the metallic substrate. The Al-Si oxide film behavior has been examined during the tensile testing.

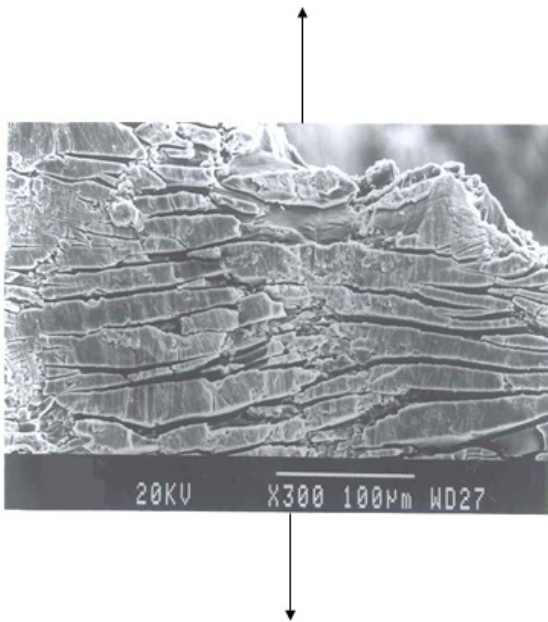


Figure 5. Partial section image of an oxide film produced by direct current (sample AlSiDC1) after tension testing.

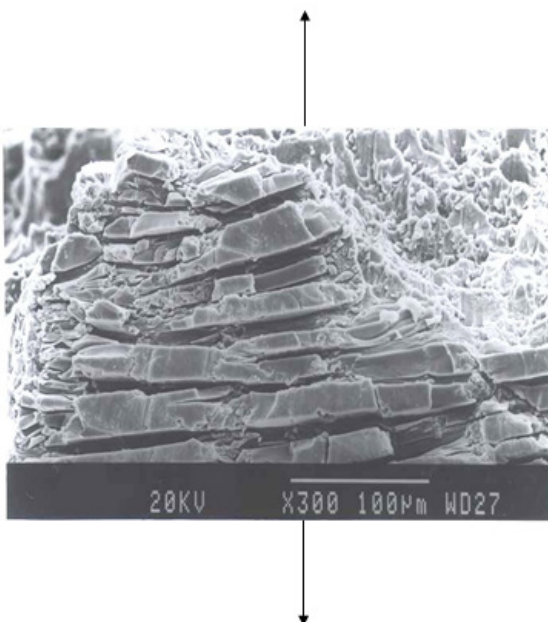


Figure 6. Partial section image of an oxide film produced by pulsed current (sample AlSiPC1) after tension testing.

In this study, an analysis was performed (by tension testing) to determine the time at which the oxide film starts cracking. Samples were subjected to strain on a tensile testing machine. A tension test specimen was subjected to multiple straining processes, and its surface was examined using an optical microscope afterwards to ascertain its cracking time. The first strain applied on the sample was 0.1%. Under 0.1% of strain, there was a crack on the oxide film surface. The aforementioned sample surface was analyzed, as shown in Figures 7 and 8, through which cracks in the oxide layer can be clearly observed.

The oxide films developed by pulsed and direct current were fractured under 0.1% of strain, which indicates that anodic films grown on the Al-Si substrate were brittle, probably due to the fragile structure characteristic of an oxide film. A reduction of fatigue properties in anodized aluminum alloy 2017A was attributed to the anodic film brittleness and intermetallic particles alloying elements which results in a spread of cracks over the anodic film surface³⁴. At the beginning of the tension testing, the oxide film cracked until reaching its elastic limit due to its hardness and brittleness. Then, the Al-Si alloy underwent plastic deformation until it fractured.

4. Hardness values of anodized samples

Table 5 lists the hardness of oxide films. The values of Knoop hardness were converted into Vickers hardness using a conversion table.

As it can be seen, hardness values are very similar. This fact indicates that the type of current used for anodization has not increased the oxide films hardness on Al-Si samples. Based on Vickers hardness measurements of Al-Si substrates, it was found that their hardness is 5.56 times greater than that of the Al-Si matrix. As the two anodized samples showed the same hardness value, the oxide films of samples cracked at same strain rate (0.1%) during tension testing. According to Hemmouche, hardness is associated to an anodic film

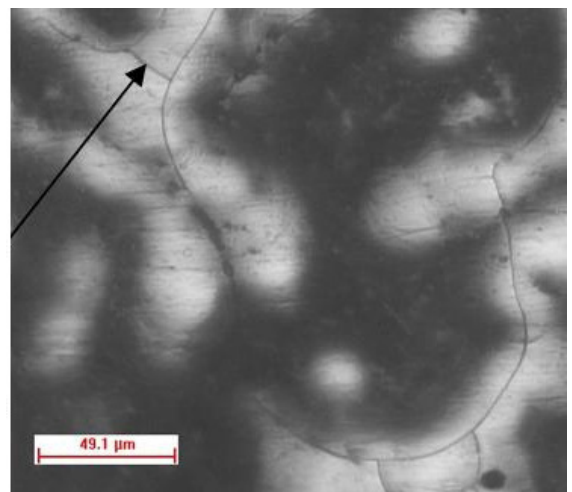


Figure 7. Optical micrograph of AlSiDC2 subjected to 0.1% of strain. The arrow indicates the cracks on the oxide film surface.

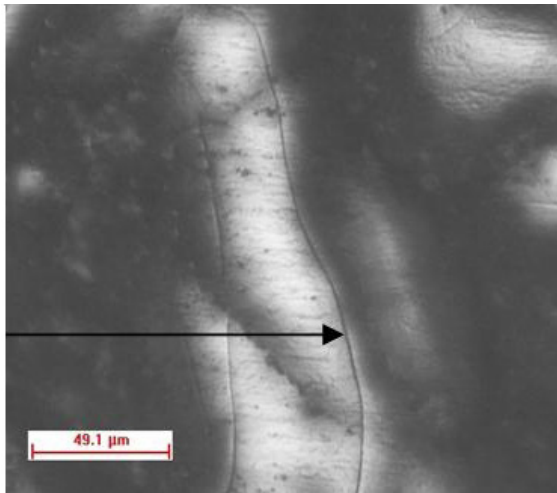


Figure 8. Optical micrograph of AlSiPC2 subjected to 0.1% of strain.

Table 5. Knoop and Vickers hardness values of the oxide film on Al-Si alloy.

Sample	Mean Knoop Hardness (HK)	Vickers Hardness (HV)
AlSiPC3	503	478
AlSiDC3	503	478
Al-Si substrate	-	86

brittleness, in which cracks started appearing over the oxide film at the beginning of the tensile process³⁴.

5. Conclusions

Anodization by pulsed current produced a more efficient oxide film whose thickness increased more constantly than that of an anodic film yielded by direct current. These results reveal that an anodization process can modify some of the mechanical properties of test specimens. The behavior of an anodized material when subjected to tension has also been analyzed herein. Microscopic analyses indicated that when an anodized material undergoes tension, its oxide film starts cracking perpendicularly to the direction of tension. It is important to note that anodized materials on Al-Si matrix should be subjected to strains of less than 0.1%, since the oxide film over Al-Si alloy cracks is under greater strain, thus exposing the substrate and making it vulnerable to deterioration. The heat treatment was efficient at obtaining a more uniform anodic film and its hardness generated by pulsed and direct current was not significantly different.

6. Acknowledgements

The authors would like to thank FAPESP for the project financial support and scholarship. Grant #1999/09110-4, São Paulo Research Foundation (FAPESP).

7. References

- Pinheiro J, Regio G, Cardoso H, Oliveira C, Ferreira J. Influence of concentration and pH of hexafluorozirconic acid on corrosion resistance of anodized AA7075-T6. *Mater Res*. 2019;22:e20190048.
- del Olmo R, Mohedano M, Visser P, Rodriguez A, Matykina E, Arrabal R. Effect of cerium (IV) on thin sulfuric acid anodizing of 2024-T3 alloy. *J Mater Res Technol*. 2021;15:3240-54.
- Fiore V, Di Franco F, Miranda R, Santamaria M, Badagliacco D, Valenza A. Effects of anodizing surface treatment on the mechanical strength of aluminum alloy 5083 to fibre reinforced composites adhesive joints. *Int J Adhes Adhes*. 2021;108:102868.
- Thompson GE, Habazaki H, Shimizu K, Sakairi M, Skeldon P, Zhou X, et al. Anodizing of aluminium alloys. *Aircr Eng Aerosp Technol*. 1999;71:228-38.
- Kwolek P, Drapała D, Krupa K, Oblój A, Tokarski T, Sieniawski J. Mechanical properties of a pulsed anodized 5005 aluminium alloy. *Surf Coat Tech*. 2020;383:125233.
- Premchand C, Hariprasad S, Saikiran A, Lokeshkumar E, Manojkumar P, Ravisankar B, et al. Assessment of corrosion and scratch resistance of plasma electrolytic oxidation and hard anodized coatings fabricated on AA7075-T6. *Trans Indian Inst Met*. 2021;74:1991-2002.
- Fratila-Apachitei LE, Duszczyc J, Katgerman L. Voltage transients and morphology of AlSi(Cu) anodic oxide layers formed in H₂SO₄ at low temperature. *Surf Coat Tech*. 2002;157:80-94.
- Raj V, Rajaram MP, Balasubramanian G, Vincent S, Kanagaraj D. Pulse anodizing - an overview. *Trans Inst Met Finish*. 2003;81:114-21.
- Mirzaei M, Bahrololoom ME. Influence of pulse currents on the nanostructure and color absorption ability of colored anodized aluminum. *Vaccum*. 2014;99:277-83.
- Regone NN, Freire CMA, Ballester M. Al-based anodic oxide films structure observation using field emission gun scanning electron microscopy. *J Mater Process Technol*. 2006;172:146-51.
- Haipeng L, Junqi Q, Changchun D. Effect of duty cycle on microstructure, composition and ablation resistance of tungsten-cobalt coatings prepared by electrodeposition. *Int J Microstruct Mater Prop*. 2019;14:256-71.
- Rossi S, Bizzotto M, Deflorian F, Fedel M. Study of anodizing process on aluminium foam to improve the corrosion behavior. *Surf Interface Anal*. 2019;51:1194-206.
- Sieber M, Morgenstern R, Lampke T. Anodic oxidation of the AlCu4Mg1 aluminium alloy with dynamic current control. *Surf Coat Tech*. 2016;302:515-22.
- Bononi M, Giovanardi R, Bozza A, Mattioli P. Pulsed current effect on hard anodizing process of 2024-T3 aluminium alloy. *Surf Coat Tech*. 2016;289:110-7.
- Bozza A, Giovanardi R, Manfredini T, Mattioli P. Pulsed current effect on hard anodizing process of 7075-T6 aluminium alloy. *Surf Coat Tech*. 2015;270:139-44.
- Zhao XX, Wei GY, Meng XF, Zhang A. High performance alumina films prepared by direct current plus pulse anodisation. *Surf Eng*. 2014;30:455-9.
- Jamaati R, Toroghinejad MR. Microstructure and mechanical properties of Al/Al₂O₃ MMC produced by anodising and cold roll bonding. *Mater Sci Technol*. 2011;27:1648-52.
- Dieter GE. Mechanical behavior of materials under tension. In: *ASM Handbook: mechanical testing and evaluation*. Materials Park: ASM International; 2000. Vol. 8; p. 20-27.
- Huang Y, Li W, Wang K. Investigation on fluidity, anodizing and tensile properties of Al-Mn alloys for application in thin-wall cast components. *Mater Res Express*. 2019;6:076571.
- Debih A, Ouakdi EH. Effect of anodization treatment on the mechanical properties and fatigue behavior of AA2017-T4 aluminum alloy Al-Cu-Mg1. *Int J Mater Res*. 2019;110:1032-8.
- Mercier S, Agogue R, Lapeyronnie P, Mavel A, Nunez P, Sinq CL. Assessment of residual performances of Al-CFRP cocured

- hybrid samples subjected to galvanic corrosion. *J Aerosp Eng*. 2019;32:04019057.
22. Yoganandan G, Balaraju JN, Manikandanath NT, Ezhilselvi V, Srivastava M, Nagacharan KV, et al. Surface and electrochemical characteristics of novel chromate-free Mn-V oxyanion sealed tartaric-sulfuric acid anodized coating. *J Mater Eng Perform*. 2018;27:6175-88.
 23. Wang L, Nie X. Silicon effects on formation of EPO oxide coatings on aluminum alloys. *Thin Solid Films*. 2006;494:211-8.
 24. Lyman T, editor. *Metals Handbook: atlas of microstructures of industrial alloys*. Metals Park: American Society for Metals; 1972. *Microstructure of aluminum alloys*; Vol. 7.
 25. Menargues S, Picas JA, Martin E, Baile MT, Campillo M, Forn A. Surface finish effect on the anodizing behaviour of Al-Si components obtained by sub-liquidus casting process. *Int J Mater Form*. 2010;3:767-70.
 26. Forn A, Picas JA, Baile MT, Martin E, García VG. Microstructure and tribological properties of anodic oxide layer formed on Al-Si alloy produced by semisolid processing. *Surf Coat Tech*. 2007;202:1139-43.
 27. Zhu B, Leisner P, Seifeddine S, Jarfors AEW. Influence of Si and cooling rate on microstructure and mechanical properties of Al-Si-Mg cast alloys. *Surf Interface Anal*. 2016;48:861-9.
 28. ASTM: American Society for Testing and Materials. ASTM E8M-01: standard test methods for tension testing of metallic materials [metric]. West Conshohocken: ASTM; 2001.
 29. Samuel AM, Elgallad EM, Doty HW, Valtierra S, Samuel FH. Effect of metallurgical parameters on the microstructure, hardness impact properties, and fractography of Al-(6.5–11.5) wt % Si based alloys. *Mater Des*. 2016;107:426-39.
 30. Din SU, Kamran J, Hasan BA, Tariq NH, Mehmood M, Zuha MSU. Effect of thermo mechanical treatments and aging parameters on mechanical properties of Al- Mg-Si alloy containing 3 wt. %. *Li Mater Des*. 2014;64:366-73.
 31. Romios M, Tiraschi R, Parrish C, Babel HW, Ogren JR, Es-Said OS. Design of multistep aging treatments of 2099 (C458) Al-Li alloy. *J Mater Eng Perform*. 2005;14:641-6.
 32. Li J, Cheng X, Li Z, Zong X, Zhang SQ, Wang HM. Improving the mechanical properties of Al-5Si-1Cu-Mg aluminum alloy produced by laser additive manufacturing with post-process heat treatments. *Mater Sci Eng A*. 2018;735:408-17.
 33. Umezawa O, Nagai K. Microstructural refinement of an As-Cast Al-12.6 Wt Pct Si alloy by repeated thermomechanical treatment to produce a heavily deformable material. *Metall Mater Trans, A Phys Metall Mater Sci*. 1999;30:2221-8.
 34. Hemmouche L, Fares C, Belouchrani MA. Influence of heat treatments and anodization on fatigue life of 2017A alloy. *Eng Fail Anal*. 2013;35:554-61.